

Geophysical Research Letters®



RESEARCH LETTER

10.1029/2023GL103505

Gravity Data Allow to Image the Shallow-Medium Subsurface Below Mud Volcanoes

Massimo Nespoli¹ , Marco Antonellini² , Dario Albarello³, Matteo Lupi⁴ , Nicola Cenni¹ , and Antonello Piombo¹ 

¹Department of Physics and Astronomy “Augusto Righi”, Alma Mater Studiorum - Università di Bologna, Bologna, Italy, ²Department of Biological, Geological, and Environmental Sciences, Alma Mater Studiorum - Università di Bologna, Bologna, Italy, ³Department of Physical Sciences, Earth and Environment, Università di Siena, Siena, Italy, ⁴Department of Earth Sciences, University of Geneva, Geneva, Switzerland

Key Points:

- A microgravimetric survey coupled with laboratory density measurements allows to image the shallow to medium subsurface below mud volcanoes
- Gravimetric data allow to distinguish between morphologies due to caldera collapse and the surface expression of slip along a fault
- For the first time the attenuation volume caused by mud intrusion is imaged by gravimetry along a fault

Supporting Information:

Supporting Information may be found in the online version of this article.

Correspondence to:

M. Nespoli,
massimo.nespoli2@unibo.it

Citation:

Nespoli, M., Antonellini, M., Albarello, D., Lupi, M., Cenni, N., & Piombo, A. (2023). Gravity data allow to image the shallow-medium subsurface below mud volcanoes. *Geophysical Research Letters*, 50, e2023GL103505. <https://doi.org/10.1029/2023GL103505>

Received 3 MAR 2023

Accepted 30 SEP 2023

Author Contributions:

Conceptualization: Massimo Nespoli, Marco Antonellini, Dario Albarello, Matteo Lupi, Antonello Piombo
Data curation: Massimo Nespoli, Nicola Cenni, Antonello Piombo
Funding acquisition: Antonello Piombo
Investigation: Nicola Cenni, Antonello Piombo
Methodology: Massimo Nespoli, Marco Antonellini, Dario Albarello, Matteo Lupi, Nicola Cenni, Antonello Piombo
Software: Massimo Nespoli
Supervision: Antonello Piombo

Abstract The debate about the conceptual model of mud volcanoes functioning is still alive in the literature. A large part of the literature focuses on the characterization of the deep reservoir where expelled fluids are expected to originate. Another part of literature is focused on the study of the shallow system of mud volcanoes, which could influence the short-term variations in mud volcanoes activity. We present and analyze a new data set of micro-gravimetric data to study the area of the *Nirano Salse*, Italy. Unlike what is commonly assumed for the study area, our results suggest that the geomorphology of the *Nirano Salse* is not related to a caldera collapse above a shallow mud chamber, but to the surface expression of slip distribution of a fault termination along which the fluids ascended to the surface. We believe that gravimetric data can significantly improve the study of hydrocarbon seeps and mud volcanism.

Plain Language Summary Mud volcanoes are broadly distributed throughout the globe, both on-and off-shore. They are formed by the episodic eruption of mud and rock fragments. The eruptions are mainly driven by of gravitative instability, due to the overall low density of clay on surrounding soil types and fluid overpressures. To date, a physical conceptual model of the area of *Nirano Salse* (Northern Italy), ascribes the mud eruptions to the presence of over-pressurized fluids that are expelled from a main deep reservoir. The latter is put into communication with the surface due to the episodic reactivation of pre-existing faults or pipes. The debate about this conceptual model is still open. To improve it, a new data set of gravimetric data was acquired during 2022. Our results suggest that the morphology of the study area is due to the presence of an almost vertical fault, which acts as a preferential route for the ascent of deep fluids.

1. Introduction

Hydrocarbon seeps and mud volcanoes are fluid-releasing geological structures observed both on-and off-shore (Etiopie, 2015; Kopf, 2002; Martinelli & Panahi, 2006; Mauri, Husein, Mazzini, Irawan, et al., 2018; Mazzini et al., 2023; Milkov, 2000; Revil, 2002). Because of the association with hydrocarbon reservoirs, they raise interesting scientific questions about their formation and behavior. To date, mud volcanic hazard is underestimated as shown by recent mud eruptions. In 1997 the eruption of the Piparo mud volcano (Island of Trinidad) buried roads and houses, damaged electrical and water infrastructures and killed animals and livestock (Blake et al., 2021). In 2014, the violent and unexpected eruption of the *Macalube di Aragona* mud volcano, (Italy) caused two fatalities (Gattuso et al., 2021; Napoli et al., 2020). For these reasons, the understanding of the mechanisms driving mud volcanism is important for hazard assessment evaluation. Furthermore, as mud volcanoes and gas seeps emit significant quantities of methane, their study is important for the correct calculation of the natural greenhouse gas emissions budget (Etiopie & Milkov, 2004; Etiopie & Schwietzke, 2019; Vannoli et al., 2021).

Mud volcanoes are formed by the episodic eruption of mud breccia or mud slurries, which are expelled at the Earth's surface by buoyancy and overpressure (Mazzini & Etiopie, 2017). The buoyancy can be due to a gravitative instability, which arises from the lower density of fluid-rich clay lithologies. Mud volcanoes are dynamic and stress-sensitive geological systems (e.g., Lupi et al., 2015; Martinelli & Judd, 2004; C. Wang & Manga, 2021). Bonini (2012) and Buttitta et al. (2020) suggest that the regional stress field can have an important role in regulating the eruption. In fact, mud volcanoes and hydrocarbon seeps usually occur in compressional settings which favor the increase of pore-pressure, therefore, facilitating the eruption of fluidized material. The ascent of fluids

© 2023. The Authors.

This is an open access article under the terms of the [Creative Commons Attribution License](https://creativecommons.org/licenses/by/4.0/), which permits use, distribution and reproduction in any medium, provided the original work is properly cited.

Writing – original draft: Massimo Nespoli, Marco Antonellini, Dario Albarello, Matteo Lupi, Antonello Piombo

Writing – review & editing: Massimo Nespoli, Marco Antonellini, Dario Albarello, Matteo Lupi, Antonello Piombo

is also favored by the presence of faults, which can act as preferential pathways for the ascent of these deep fluids (Mazzini, 2009).

In Italy, mud volcanoes are characterized by the almost continuous, but relatively quiet, expulsion of material (Giambastiani et al., 2022). In the present work we focus on the mud volcanoes located in the northern Apennines Italy (e.g., Borgatti et al., 2019; Capozzi & Picotti, 2002), near the city of Fiorano Modenese (Emilia-Romagna region). Such volcanoes, belonging to the Regional Natural Reserve of *Nirano Salse* are well known since ancient times and attract thousands of visitors every year. To date, the physical conceptual model of the *Nirano Salse* ascribes the eruptions to the presence of overpressurized fluids that are expelled from a leaky deep reservoir (Bonini, 2008).

In general, most studies devoted to the characterization of the *Nirano Salse* focus on the deep reservoir where expelled fluids originate (e.g., Martinelli et al., 2012; Oppo et al., 2017; Sciarra et al., 2019). However, much more important to characterize short term variations in gas-mud emissions activity might be the presence of shallow depth secondary reservoirs. Within them, gas and connate water coming from depth may accumulate and remain at rest until overpressure building up opens the conduits to the surface. According to Giambastiani et al. (2022) and ref. therein, the reservoirs are put into communication with the surface due to the episodic reactivation of pre-existing faults or pipes. In this view, Lupi et al. (2015) and Giambastiani et al. (2022) also underline the importance of the shallow aquifers (tens of meters of depth), which may act as buffers where rising gas (methane) is trapped and temporarily stored. This configuration could lead to the localization of small groups of gryphons, mud pools, and mud cones (Figure 1a) just above the shallow reservoirs.

This view suggests that small scale geophysical surveys could be determinant for the identification of these shallow reservoirs or of a large mud caldera at shallow surface below the whole Nirano area as suggested by Bonini (2008, 2009, 2020). The implications for unraveling the subsurface structure are important to evaluate potential hazards at different spatial scales connected to the fluid emissions. Short scale resistivity surveys were carried out in the Nirano area (e.g., Accaino et al., 2007; Lupi et al., 2015; Romano et al., 2023) also integrated with geochemical methods (e.g., Martinelli et al., 2012; Oppo et al., 2017; Sciarra et al., 2019). To better understand the conceptual model of fluids, rise and storage as well as the subsurface structural setting of Nirano a new data set of gravimetric data is here presented. The gravimetric data can be valuable in distinguishing the volumes characterized by a high gas/fluid saturation (i.e., low density) from the hosting materials with higher density. Gravity surveys performed in mud volcanoes zones (e.g., Kadirov et al., 2005; Mauri, Husein, Mazzini, Irawan, et al., 2018; Mauri, Husein, Mazzini, Karyono, et al., 2018; Napoli et al., 2020; Odone et al., 2021; Riffo et al., 2021; Sayyadul, 2005) are useful to constrain the actual location of gas saturated volumes. We show that they can also give important information about the mechanisms that influenced the actual Nirano morphology and provide guidance about hazards of mud-fluid emissions in the area.

1.1. Geological Setting

The *Nirano Salse* are located at the foothills of the Northern Apennines (Figure 1) in an area where Plio-Pleistocene transgressive clays (Argille Azzurre Fm, FAA) blanket the surface down to a depth of 50–150 m. Below this clay unit, a series of Miocene to Oligocene marly and sandy deposits (Termina Fm—sand, Pantano Fm—sand/marl turbidites, Antognola Fm—marls, and Ranzano Fm—sand; Gasperi et al., 2005) form a stratigraphic package of 1,000–1,500 m in thickness. The lithostratigraphic series continues with Cretaceous-Eocene Ligurian clay units constituting the basement of the sequence. The Miocene-Oligocene units are crosscut by a series of high angle faults and fracture zones with a NW-SE and NE-SW orientations (Gasperi et al., 2005). No brittle structures, however, are observed in the upper FAA. The mud volcanic features in the area consist of mud pools, gryphons, and dry seeps (Figures 1a and 1b) (Etioppe, 2015), which are located within a geomorphological depression. Bonini (2008, 2009) argued a collapse of a shallow mud filled caldera along bordering ring faults and the presence of an anticline just above the depression (Bonini, 2007). Field evidence and the published geologic map of Gasperi et al. (2005), however, do not show an anticline but the hinge of a monocline (Figure 1). More recently, Bonini (2020) and Maestrelli et al. (2019) stressed the importance of far structures and near structures in controlling fluid ascent in the compressional setting of the Northern Apennines defining two separate structural and reservoir systems (deep source and shallow source reservoirs), which would be present also in the Nirano area.

Field mapping, structural planes attitudes measurements, and sampling were also performed during the geophysical field study to integrate the existing information. In particular, rock saturated density was determined on 18

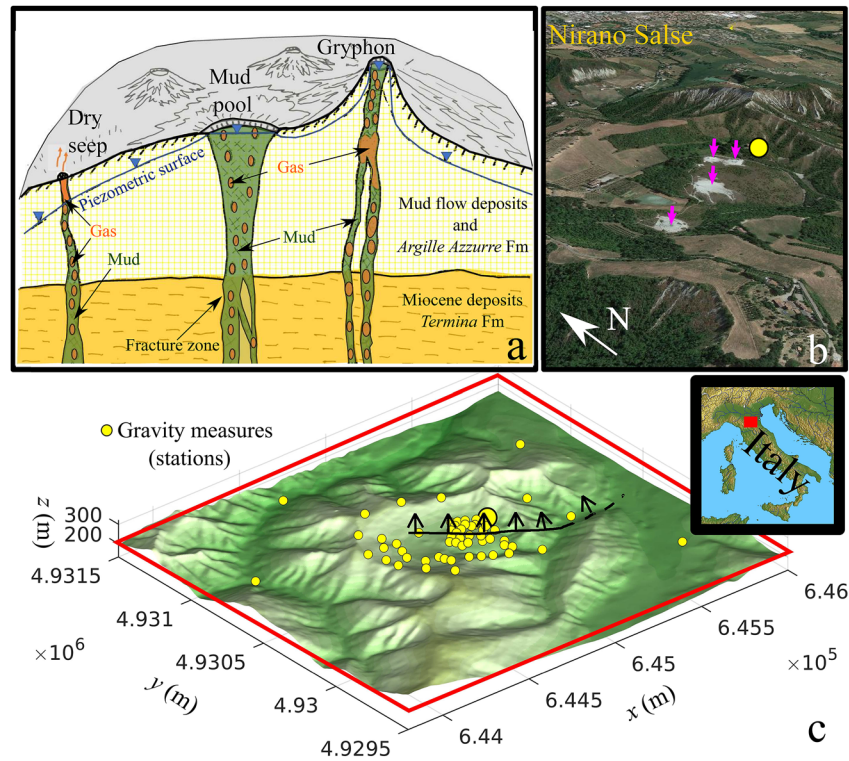


Figure 1. Illustration of the study area. (a) Sketch of the main features of the study area. (b) Aerial image view of the study area (Image Landsat-Copernicus, Google). Magenta arrows indicate the four gryphons. (c) Zoom on the study area: the yellow circles represent the gravity stations. The biggest one represents the reference base station. The black line indicates the trace of the monocline as inferred by the present work.

samples of the FAA, Termina, and Pantano Fm by fluid immersion with the British Standard Institution method BS 1377:1975 Test 6 (BS, 1975). Density ranges 1,680–1,950 kg/m³ for the FAA, 2,150–2,180 kg/m³ for the Termina Fm, and 2,220–2,320 kg/m³ for the Pantano Fm (Table S1 in Supporting Information S1).

2. Material and Methods

The data set was acquired during a field campaign performed in 2022. The measures were obtained with a LaCoste-Romberg Model D-149 relative gravimeter in 61 different stations (Figure 1c) distributed over an area of about 4 km² and centered on the mud volcanoes zone. The reference point of the data set is reported in Figure 1c. The altitudes of gravity measurement stations were obtained with leveling in the central zone (Leica Sprinter 250M) whereas the farthest points were measured with GPS-RTK (Leica CS15).

The regional Digital Elevation Model (DEM) (Figure S1 in Supporting Information S1) has a resolution of 5 m × 5 m (<https://geoportale.regione.emilia-romagna.it>) and it was used to compute the terrain correction. The mean value of gravity, g_i^{obs} , at each observation station, i , was first corrected in order to account for the tides contribution and the drift rate of the instrument (e.g., McCubbine et al., 2018; Reilly, 1970). For each location, i , we also consider the latitude correction $g_i^n(\lambda_i)$, the free-air correction δg_i^{FA} and the Bouguer correction δg_i^{B} (see Supporting Information S1 for further details). For the latter, we assume a density of the plate of $\rho = 1,850 \text{ kg/m}^3$, that is the average density of the shallow lithologic units making up the stratigraphic sequence of the area (Table S1 in Supporting Information S1). The free air Δg_i^{FA} and the Bouguer Δg_i^{B} anomalies can be then computed respectively, as following:

$$\Delta g_i^{\text{FA}} = g_i^{\text{obs}} - g_i^n + \delta g_i^{\text{FA}} \quad (1)$$

$$\Delta g_i^{\text{B}} = g_i^{\text{obs}} - g_i^n + \delta g_i^{\text{FA}} - \delta g_i^{\text{B}} \quad (2)$$

Due to the complex topography of the study area, the terrain correction for each location, Δg_i^{T} , was also computed. Its computation was performed with the prism method (e.g., Almeida et al., 2018; Nagy, 1966) considering the

regional DEM shown in Figure S1 in Supporting Information S1 and compared with another independent method (Hammer, 1939). The complete Bouguer anomaly can be then computed as

$$\Delta g_i^{CB} = \Delta g_i^B + \Delta g_i^T \quad (3)$$

Relative free air, Δg_i^{RFA} , Bouguer and Δg_i^{RB} anomalies, as well as the relative terrain correction Δg_i^{RT} , with respect to the reference location REF (Figure 1c), can be computed respectively as following

$$\Delta g_i^{RFA} = \Delta g_i^{FA} - \Delta g^{FA(REF)}, \quad (4)$$

$$\Delta g_i^{RB} = \Delta g_i^B - \Delta g^{B(REF)}, \quad (5)$$

$$\Delta g_i^{RT} = \Delta g_i^T - \Delta g^{T(REF)}. \quad (6)$$

The resulting Δg_i^{RFA} , Δg_i^{RT} , and Δg_i^{RB} are plotted in Figures 2c–2e, respectively. In the same way, we can compute the relative, complete Bouguer anomaly (Figure 2f) as

$$\Delta g_i^{RCB} = \Delta g_i^{CB} - \Delta g^{CB(REF)}. \quad (7)$$

As we can see from Figure 2d, the terrain correction has a minimum close to the mud volcanoes due to the flat topography of this area. The complete Bouguer anomaly will be considered in the following data inversion process.

3. Inversion of Gravity Data

The 3D inversion for density contrasts was performed with the GROWTH 3.0 software (Camacho et al., 2021), which allows to determine the subsurface density distribution starting from discrete gravity anomaly observations. The inversion was performed in a 3D domain (32,171 cells), which encompasses the distribution of all measurement stations and a depth of 403 m (a.m.s.l.). We used as input data the complete Bouguer anomaly, Δg_i^{RCB} shown in Figure 2f. The offset O_j was estimated by the inversion as $O_j = -210 \mu\text{Gal}$.

The resulting complete Bouguer anomaly, after the removal of the offset, is shown in Figure 3a. Anomalies range from about -1.5 to 1.5 mGal in the whole study area. The strongest negative anomaly of about 1.5 mGal is located just below the four mud volcanoes and in the southeast part of the study area. Positive anomalies up to 1.5 mGal are located to the southwest of the mud volcanoes. The trade-off curve used to select the smoothing parameter (Camacho et al., 2021) is shown in Figure S3 of Supporting Information S1. The model sensitivity (Figure S4 in Supporting Information S1) is higher in the vicinity of the area hosting the mud volcanoes, where the distribution of stations is finer. The resolution tests (Figure S5 in Supporting Information S1) indicate that our distribution of the stations is suitable to resolve anomalous density volumes with a size (width and depth) of the order of some hundreds of meters.

The subsurface density anomalies retrieved by the inversion are reported in Figures 3b–3d. Results suggest the presence of a volume ($\sim 2 \times 10^8 \text{ m}^3$) with an anomalous negative density contrast up to about -350 kg/m^3 , located below the mud volcanoes. Such a volume extends from a few meters below the surface down to about 400 m depth. From the map section plotted at $z = 50$ m (Figure 3b), the N-S vertical section AA' (Figure 3c), and the BB' vertical section (Figure 3d) we identify some volumes with positive density contrast up to about $+350 \text{ kg/m}^3$. The inferred positive density contrasts extend from a few meters below the surface (about 200 a.m.s.l.) down to about 0 m (a.m.s.l.) elevation. The residuals between measured and modeled Bouguer gravity anomalies are generally low except for a few stations (Figure S1 in Supporting Information S1).

4. Discussion

The Bouguer anomaly map (Figure 3a) shows a low-density anomaly (about $-1,500 \mu\text{Gal}$) striking in a NW-SE direction that terminates to the NW where a high-density anomaly (about $+1,500 \mu\text{Gal}$) is observed. The tip of the anomaly termination corresponds to the region where three different groups of gryphons and mud pools are observed at the surface (Figure 3a). Published geological maps and interpretations (Bonini, 2008; Gasperi et al., 2005) report the axis of an anticline at the same location of the low-density anomaly. Field mapping

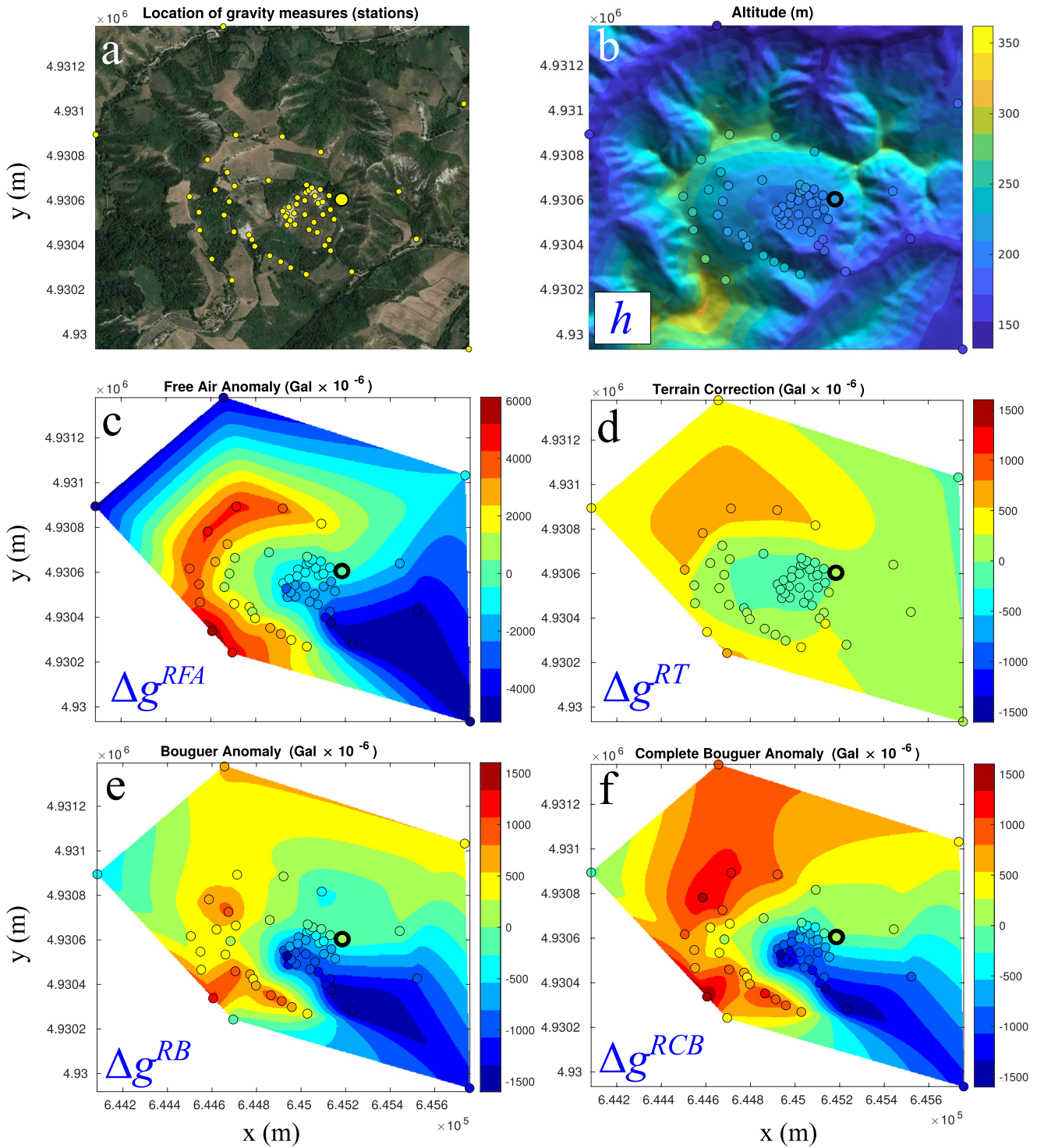


Figure 2. Gravity data analysis. Circles represent the location of the gravity measures (stations). (a) Locations of the stations. The greatest circle is the reference station. (b) Altitude from DEM; (c) Relative free air anomaly, Δg_i^{RFA} ; (d) Terrain Correction, Δg_i^{RT} ; (e) Bouguer Anomaly Δg_i^{RB} ; (f) complete Bouguer anomaly Δg_i^{RCB} .

performed during our work, pointed out only the presence of a NW-SE oriented monocline axis marking a steepening of the strata north of the mud volcanoes in the ductile clays of the FAA. The direction of the Bouguer low-density anomaly corresponds to the strike of the monocline axis and of the NW-SE oriented subvertical

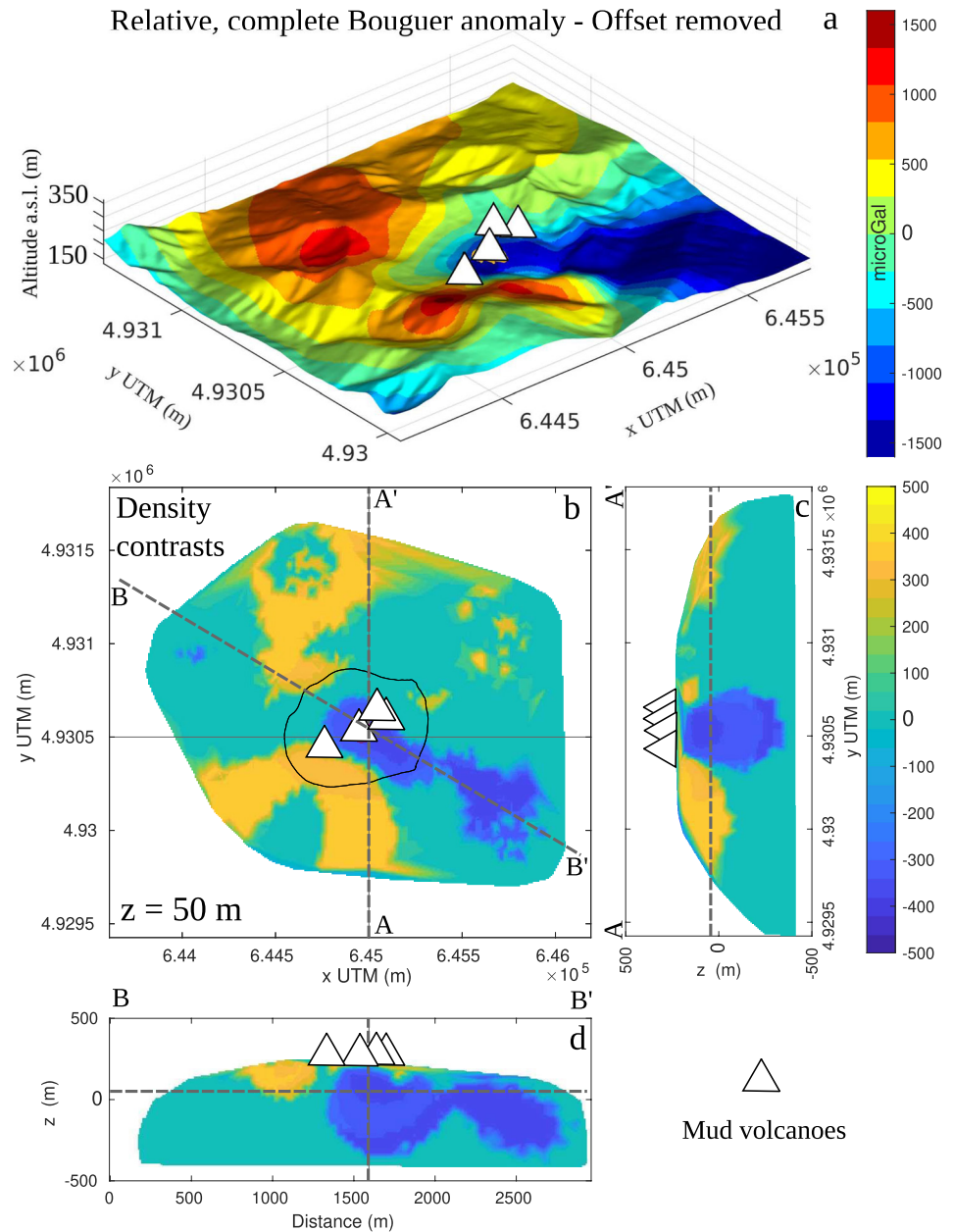


Figure 3. (a) Relative, complete Bouguer anomaly without offset estimated by the inversion procedure. (b-d) Results of the inversion for density contrasts performed with GROWTH 3.0 (Camacho et al., 2021). Plot of $\Delta\rho$ on a horizontal section at $z = 50$ m, the black line includes the area of mud volcanoes, the dashed gray lines indicate the traces of the AA' and BB' sections (b); vertical N-S (c) and NW-SE section (d).

faults. The latter, that are present just south of the Nirano area in the exposed Miocene sequence covered by the transgressive FAA clays, have offsets ranging from a few meters to a few hundred meters (Gasperi et al., 2005).

Even if the resolution of the model used for the inversion of the gravity data does not allow to see the shallow, very small-scale (tens of meters) details of the study area, it has allowed us to reveal the main structures that characterize the study area on larger spatial scales (hundreds of meters). The gravity inversion results (Figures 3b–3d) define a NW-SE oriented low-density zone with $\rho \approx 1,500\text{--}1,600$ kg/m³ and a density contrast $\Delta\rho \approx -350$ kg/m³ with respect to the average density of the surface clays (1,850 kg/m³) used in the inversion. Such a low-density zone has a width of about 200 m and a length of about 1,300 m (Figure 3b). It extends from beneath the topographic surface (about 200 m.a.s.l.) down to about -300 m.a.s.l. (Figures 3c and 3d). Considering that the

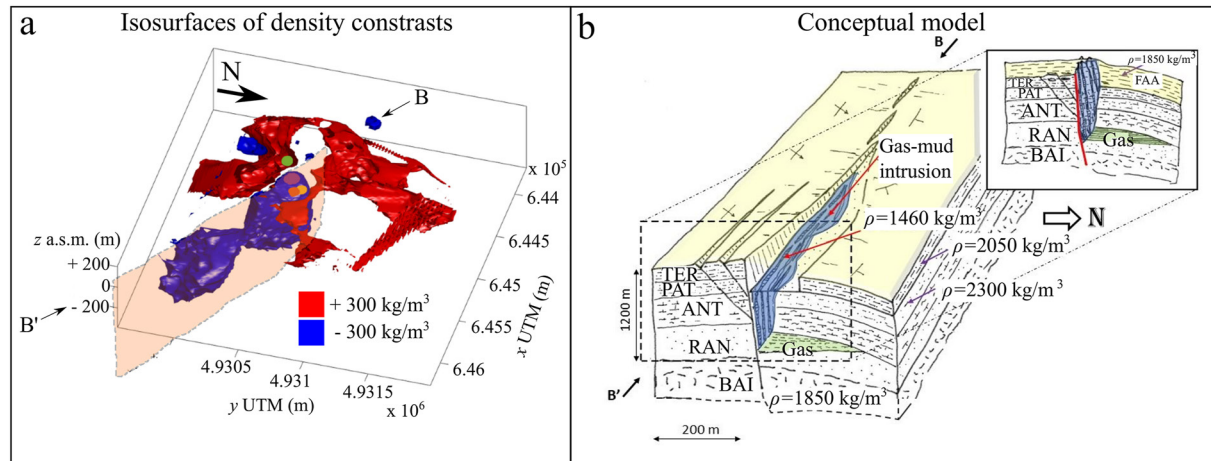


Figure 4. (a) Isosurfaces computed for density contrasts $|\Delta\rho| = 300 \text{ kg/m}^3$. The orange plane represents the fault. (b) Conceptual model showing the different geological structures: the fault termination with a steep slip gradient, the monocline, the mud/gas intrusion in the fault zone, and some ancillary faults are also shown. BAI are clay breccias of Ligurian origin (Eocene), RAN is the Ranzano Fm (Oligocene-Miocene), ANT is the Antognola Fm (Miocene), PAT is the Pantano Fm (Miocene), TER is the Termina Fm (Miocene), FAA are the Argille Azzurre Fm (Pliocene-Pleistocene); this latter formation (light yellow) has been removed in the 3D conceptual model to show the top of the deformed Miocene. The inset of panel (b) shows a cross section. Light green is gas, light blue is the zone of mud/gas intrusion into the fault zone. Density values are also reported.

average density of the Miocene rocks from 100 m down to a depth of 1,000 m from the surface is around 2,000–2,200 kg/m^3 , the low-density zone may be interpreted as the result of gas and/or mud saturation in a rock with a large amount of matrix or fracture porosity (e.g., Mauri, Husein, Mazzini, Irawan, et al., 2018; Mauri, Husein, Mazzini, Karyono, et al., 2018), or by intrusion of viscous mud-gas slurry dykes. Given that in the Nirano area the geothermal gradient is normal (25 K/km, Viganò et al., 2012), the methane down to a depth of 700–800 m from the surface would be in gaseous form and, eventually, in supercritical state only at the bottom of the low-density zone (McCain, 1990). In these conditions, the low-density zone is compatible with a rock of the Miocene sequence having a gas-saturated porosity in the order of 30%–40%. This would be possible in the damage zone of a fault with large matrix and fracture porosity or where some fluid filled mud/gas cracks and feeders intruded the rock. Considering the densities of both mud ($\rho = 1,200 \text{ kg/m}^3$, Giambastiani et al., 2022) and rocks, and the gas content within them, we can easily obtain the inferred density anomalies assuming volumetric ratios (volume of gas/volume of mud and/or rock) in the range 0.55–0.70. By examining the isosurfaces computed for density contrasts $|\Delta\rho| = 300 \text{ kg/m}^3$ in the inverted gravity model (Figure 4a), we can infer that: (a) there is a low-density zone ($\Delta\rho = -300 \text{ kg/m}^3$), which is laying on a vertical NW-SE striking plane and (b) the top of the high density zone ($\Delta\rho = +300 \text{ kg/m}^3$), which forms a flexure, is structurally higher in the South-SW than in the North-NE area. Although the NE area is constrained by a lower number of stations with respect to the SW area, the presence of a strong positive density anomaly in the SW area is coherent with the high Bouguer anomaly observed there (Figure 2f).

We interpret the top of the high-density zone as the top of the Miocene marly formations that have densities compatible with those obtained in the inversion. These features could be the result of gas/mud intrusion along a NW-SE oriented vertical fault zone whose displacement is diminishing in the NW direction. This conceptual model, which is represented in Figure 4b, is coherent with the structural frame of the area (Gasperi et al., 2005), the density values measured in the rocks of the sedimentary sequence, the surface geology and morphology. The offset of the fault, based on the thickness of the sedimentary sequence, is in the order of 100–150 m with a down-to the NE-throw. As the low-density zone terminates at a depth from the surface of about 800 m, we suppose that the gas reservoir is located within the Ranzano Fm, as also suggested by Capozzi and Picotti (2002). This reservoir would correspond to the shallow reservoir buffering deep ascending gas, which was proposed in Bonini (2020) model. At the Nirano reservoir, gas likely escaped updip at the termination or in the linkage zone of a fault above a poorly sealed reservoir (Knipe, 1997). The gas leaked into the FAA probably in association with over-pressured mud dykes (Tingay et al., 2009) and/or directly into the fractured porosity of the fault damage zone. Similar situations of mud diapirism and intrusion along fault zones have been described also by Bonini (2020), MacDonald et al. (2000), Mazzini and Etiope (2017), Orange et al. (1999), Y.

Wang et al. (2022), and Zhong et al. (2021). The gravity data that we present, however, are not in agreement with the seismic line interpretation presented in Maestrelli et al. (2019) who at 0.5–0.6 s depth still interpret the reflectors in the sequence as belonging to the FAA; we believe that those reflectors are within the Miocene sequence where there is enough significant contrast in acoustic impedance. The homogeneous FAA, on the other hand, would not cause any reflection. With reflectors within the Miocene, our gravity data interpretation would be coherent with the one of the seismic data (Maestrelli et al., 2019). The conceptual structural model that we present, however, concerns only the upper zone above a thrust-folded area, which was investigated by the gravity survey and is not in disagreement with the deep plumbing system proposed by Maestrelli et al. (2019). The novelty of our work is to show the importance of faults in controlling mud gas emissions at the surface of the *Nirano Salse*.

Our conceptual model for the *Nirano Salse* based on the gravity data is valid down to a depth of about 1,000 m from the surface. Below that depth, we cannot exclude the existence of other deeper gas reservoirs (DR in Bonini (2020)) associated with the thrust folds of the Apennines, whose axes have the same NW-SE direction. The thrust faults proposed by Bonini (2020) could crop out in the *Argille Azzurre* Fm to the NE of the investigated area, in which case the fault that we describe could have developed from extrados fractures of a deep anticline connected to fault propagation folds (Bonini, 2020).

The geophysical results of this study also point out some important characteristics of the Nirano mud volcanism, which have implications for the safety of the reserve visitors and the local communities. First, there is no evidence of a shallow extensive mud caldera as proposed by past studies (Bonini, 2008; Sciarra et al., 2019) as the low-density zone appears to lay on a NW-SE-oriented vertical plane. Furthermore, there is no evidence of a diapir (*sensu strictu*) below the Nirano area as suggested by Oppo (2012), Bonini (2008), and Sciarra et al. (2019). The “bowl” morphology (Figure 1) so reminiscent of a caldera at Nirano does not seem to be caused by collapse along ring faults above a mud diapir or a mud chamber, but it is simply the surface expression of fault offset with a strong slip gradient toward its tip termination (Figure 4b).

The implications are that potential fluid escape structures be located along the fault zone or fracture zones (NE-SW) normal to the fault as also shown by the small isolated low-density zones in Figure 4a. These gryphons form above shallow (down to a few tens meters) mud/gas accumulations just below the vents whose plumbing system is connected to the low-density zone along the fault. Such a scenario was also suggested by hydrogeological and georesistivity surveys (Giambastiani et al., 2022; Romano et al., 2023). This information could be used to better plan access routes to the reserve and to fence off potential areas prone to sinking and subsidence.

5. Conclusions

The gravity inversion results indicate the existence of a low-density zone (1,200–1,500 m long, 100–200 m wide, 800 m deep) laying on a NW-SE-oriented vertical plane in the structural trend typical of the Northern Apennines. This zone likely represents the intrusion of fluids (mud and gas) in the damage zone of a subvertical fault, which feeds shallow fluid reservoirs (meters to a few tens of meters deep) just below the mud volcanoes both in the footwall and hanging wall of the fault. For the first time, this process is clearly documented along a fault zone. The caldera like morphology of the *Nirano Salse* summital region is not related to the presence of a mud diapir *s.s.*, or to a caldera collapse above a shallow extensive mud chamber, but to the surface expression of slip distribution at the fault termination along which the mud/gas fluids ascended to the surface. This has implications to assess better the safety of the site and the location of access points. The structure imaged by the gravity inversion has implications for the understanding of fluid flow migration along fault zones, especially where fault seal traps are involved and the combination of slip gradients, bed dips, and sealing units contribute to define the sealing risk of a geofluids reservoir. Gravity in our case was essential in testing between the caldera and fault intrusion hypotheses. This methodology, therefore, has shown to still have potential in subsurface characterization within complex structural areas.

Data Availability Statement

The gravity data are available from <https://doi.org/10.5281/zenodo.8026689>.

Acknowledgments

The authors thank Luciano Callegari, Marzia Conventi and Maria Morena for their support in the logistics and the warm welcome. This study was performed with the support from the Fiorano Modenese Municipality (Italy) and the Management Authority for Park and Biodiversity of Central Emilia (Ente di Gestione per i Parchi e la Biodiversità Emilia Centrale, Italy). The authors sincerely thank Massimo Bacchetti for his valuable contribution in planning and implementing measurement campaigns in the Salse di Nirano area and Antonino Calafato for assistance with rock density measurements. The authors would also like to thank the GEOINVEST s.r.l. team for their valuable suggestions. The authors also thank Giuliana Rossi, an anonymous reviewer and the Editor Christian Huber who greatly contributed to improve the manuscript.

References

Accaino, F., Bratus, A., Conti, S., Fontana, D., & Tinivella, U. (2007). Fluid seepage in mud volcanoes of the northern Apennines: An integrated geophysical and geological study. *Journal of Applied Geophysics*, 63(2), 90–101. <https://doi.org/10.1016/j.jappgeo.2007.06.002>

Almeida, F., Matias, M., Loureno, M., & Martins, A. (2018). A MATLAB script to perform gravity terrain corrections using DEM-EU digital elevation model in a teaching lab. In *Paper presented at 24th European Meeting of Environmental and Engineering Geophysics* (pp. 1–5). <https://doi.org/10.3997/2214-4609.201802654>

Blake, O., Ramscook, R., Iyare, U., Moonan, X., & Gopaul, R. (2021). Integrating pseudo-3D ERT and DEM to map the near-surface structures and morphology of the Piparo mud volcano, Trinidad. *Journal of Applied Geophysics*, 194, 104442. <https://doi.org/10.1016/j.jappgeo.2021.104442>

Bonini, M. (2007). Interrelations of mud volcanism, fluid venting, and thrust-anticline folding: Examples from the external northern Apennines (Emilia-Romagna, Italy). *Journal of Geophysical Research*, 112(B8), B08413. <https://doi.org/10.1029/2006JB004859>

Bonini, M. (2008). Elliptical mud volcano caldera as stress indicator in an active compressional setting (Nirano, Pede-Apennine margin, northern Italy). *Geology*, 36(2), 131–134. <https://doi.org/10.1130/G24158A.1>

Bonini, M. (2009). Mud volcano eruptions and earthquakes in the Northern Apennines and Sicily. *Italy, Tectonophysics*, 474(3–4), 723–735. <https://doi.org/10.1016/j.tecto.2009.05.018>

Bonini, M. (2012). Mud volcanoes: Indicators of stress orientation and tectonic controls. *Earth-Science Reviews*, 115(3), 121–152. <https://doi.org/10.1016/j.earscirev.2012.09.002>

Bonini, M. (2020). Investigating earthquake triggering of fluid seepage systems by dynamic and static stresses. *Earth-Science Reviews*, 210, 103343. <https://doi.org/10.1016/j.earscirev.2020.103343>

Borgatti, L., Giovanna, B., Edoardo, B. A., Stefano, C., Gloria, F., Francesca, G., et al. (2019). Evidence of late-Holocene mud-volcanic eruptions in the Modena foothills (Northern Italy). *The Holocene*, 29(6), 975–991. <https://doi.org/10.1177/0959683619831418>

BS. (1975). *BS 1377:1975:Test 6. Determination of the specific gravity of the soil particles*. British Standards Institution.

Buttitta, D., Caracausi, A., Chiaraluce, L., Favara, R., Morticelli, M. G., & Sulli, A. (2020). Continental degassing of helium in an active tectonic setting (northern Italy): The role of seismicity. *Scientific Reports*, 10(1), 162. <https://doi.org/10.1038/s41598-019-55678-7>

Camacho, A. G., Prieto, J. F., Aparicio, A., Ancochea, E., & Fernandez, J. (2021). Upgraded growth 3.0 software for structural gravity inversion and application to El Hierro (Canary Islands). *Computers & Geosciences*, 150, 104720. <https://doi.org/10.1016/j.cageo.2021.104720>

Capozzi, R., & Picotti, V. (2002). Fluid migration and origin of a mud volcano in the northern Apennines (Italy): The role of deeply rooted normal faults. *Terra Nova*, 14(5), 363–370. <https://doi.org/10.1046/j.1365-3121.2002.00430.x>

Etiopie, G. (2015). *Natural gas seepage: The Earths hydrocarbon degassing*. Springer International Publishing.

Etiopie, G., & Milkov, A. V. (2004). A new estimate of global methane flux from onshore and shallow submarine mud volcanoes to the atmosphere. *Environmental Geology*, 46(8), 997–1002. <https://doi.org/10.1007/s00254-004-1085-1>

Etiopie, G., & Schwietzke, S. (2019). Global geological methane emissions: An update of top-down and bottom-up estimates. *Elementa: Science of the Anthropocene*, 7, 47. <https://doi.org/10.1525/elementa.383>

Gasperi, G., Bettelli, G., Panini, F., & Pizziole, M. (2005). *Note illustrative della Carta Geologica d'Italia alla scala 1:50.000, foglio 219, Sassuolo, Organo Cartografico dello Stato (legge n. 68 del 2.2.1960)*. Agenzia per la protezione dell'ambiente e per i servizi tecnici (APAT) Dipartimento Difesa del Suolo; Servizio Geologico d'Italia; Progetto CARG.

Gattuso, A., Italiano, F., Capasso, G., D'Alessandro, A., Grassa, F., Pisciotta, A. F., & Romano, D. (2021). The mud volcanoes at Santa Barbara and Aragona (Sicily, Italy): A contribution to risk assessment. *Natural Hazards and Earth System Sciences*, 21(11), 3407–3419. <https://doi.org/10.5194/nhess-21-3407-2021>

Giambastiani, B. M. S., Antonellini, M., Nespoli, M., Bacchetti, M., Calafato, A., Conventi, M., et al. (2022). Mud flow dynamics at gas seeps (Nirano Salse, Italy). *Environmental Earth Sciences*, 81(19), 480. <https://doi.org/10.1007/s12665-022-10615-2>

Hammer, S. (1939). Terrain correction for gravimeter stations. *Geophysics*, 4(3), 149–230. <https://doi.org/10.1190/1.1440495>

Kadirov, F. A., Lerche, I., Guliyev, I. S., Kadyrov, A. G., Feyzullayev, A. A., & Mukhtarov, A. S. (2005). Deep structure model and dynamics of mud volcanoes, southwest Absheron Peninsula (Azerbaijan). *Energy Exploration and Exploitation*, 23(5), 307–332. <https://doi.org/10.1260/01445980577599271>

Knipe, R. J. (1997). Juxtaposition and seal diagrams to help analyze fault seals in hydrocarbon reservoirs. *AAPG Bulletin*, 81(2), 187–195. <https://doi.org/10.1306/522B42DF-1727-11D7-8645000102C1865D>

Kopf, A. J. (2002). Significance of mud volcanism. *Reviews of Geophysics*, 40(2), 2-1–2-52. <https://doi.org/10.1029/2000RG000093>

Lupi, M., Ricci, B. S., Kenkel, J., Ricci, T., Fuchs, F., Miller, S. A., & Kemna, A. (2015). Subsurface fluid distribution and possible seismic precursory signal at the Salse di Nirano mud volcanic field, Italy. *Geophysical Journal International*, 204(2), 907–917. <https://doi.org/10.1093/gji/ggv454>

MacDonald, I. R., Buthman, D. B., Sager, W. W., Peccini, M. B., & Guinasso, N. L. (2000). Pulsed oil discharge from a mud volcano. *Geology*, 28(10), 907–910. [https://doi.org/10.1130/0091-7613\(2000\)28<907:PODFAM>2.0.CO;2](https://doi.org/10.1130/0091-7613(2000)28<907:PODFAM>2.0.CO;2)

Maestrelli, D., Bonini, M., & Sani, F. (2019). Linking structures with the genesis and activity of mud volcanoes: Examples from Emilia and Marche (Northern Apennines, Italy). *International Journal of Earth Sciences*, 108(5), 1683–1703. <https://doi.org/10.1007/s00531-019-01730-w>

Martinelli, G., Cremonini, S., & Samonati, E. (2012). Geological and geochemical setting of natural hydrocarbon emissions in Italy. In H. A. Al-Megren (Ed.), *Advances in Natural Gas Technology*. IntechOpen. Chapter 4.

Martinelli, G., & Judd, A. (2004). Mud volcanoes of Italy. *Geological Journal*, 39(1), 49–61. <https://doi.org/10.1002/gj.943>

Martinelli, G., & Panahi, B. (2006). Mud volcanoes, geodynamics and seismicity. In *Proceedings of the NATO Advanced Research Workshop on Mud Volcanism, Geodynamics and Seismicity, Baku, Azerbaijan, from 20 to 22 May 2003. NATO Science Series* (Vol. 4). Springer Netherlands.

Mauri, G., Husein, A., Mazzini, A., Irawan, D., Sohrabi, R., Hadi, S., et al. (2018). Insights on the structure of Lusi mud edifice from land gravity data. *Marine and Petroleum Geology*, 90, 104–115. <https://doi.org/10.1016/j.marpetgeo.2017.05.041>

Mauri, G., Husein, A., Mazzini, A., Karyono, K., Obermann, A., Bertrand, G., et al. (2018). Constraints on density changes in the funnel-shaped caldera inferred from gravity monitoring of the Lusi mud eruption. *Marine and Petroleum Geology*, 90, 91–103. <https://doi.org/10.1016/j.marpetgeo.2017.06.030>

Mazzini, A. (2009). Mud volcanism: Processes and implications. *Marine and Petroleum Geology*, 26(9), 1677–1680. <https://doi.org/10.1016/j.marpetgeo.2009.05.003>

Mazzini, A., & Etiopie, G. (2017). Mud volcanism: An updated review. *Earth-Science Reviews*, 168, 81–112. <https://doi.org/10.1016/j.earscirev.2017.03.001>

Mazzini, A., Sciarra, A., Lupi, M., Ascough, P., Akhmanov, G., Karyono, K., & Husein, A. (2023). Deep fluids migration and submarine emersion of the Kalang Anyar mud volcano (Java, Indonesia): A multidisciplinary study. *Marine and Petroleum Geology*, 148, 105970. <https://doi.org/10.1016/j.marpetgeo.2022.105970>

- McCain, W. D. (1990). *The properties of petroleum fluids* (2nd ed.). PennWell Books, PennWell Publishing Company.
- McCubbine, J., Tontini, F. C., Stagpoole, V., Smith, E., & OBrien, G. (2018). Gsolve, a python computer program with a graphical user interface to transform relative gravity survey measurements to absolute gravity values and gravity anomalies. *SoftwareX*, 7, 129–137. <https://doi.org/10.1016/j.softx.2018.04.003>
- Milkov, A. (2000). Worldwide distribution of submarine mud volcanoes and associated gas hydrates. *Marine Geology*, 167(1), 29–42. [https://doi.org/10.1016/S0025-3227\(00\)00022-0](https://doi.org/10.1016/S0025-3227(00)00022-0)
- Nagy, D. (1966). The prism method for terrain corrections using digital computers. *Pure and Applied Geophysics*, 63(1), 31–39. <https://doi.org/10.1007/BF00875156>
- Napoli, R., Currenti, G., Giammanco, S., Greco, F., & Maucourant, S. (2020). Imaging the salinelle mud volcanoes (Sicily, Italy) using integrated geophysical and geochemical survey. *Annals of Geophysics*, 63(4), 442. <https://doi.org/10.4401/ag-8215>
- Odonne, F., Imbert, P., Remy, D., Gabalda, G., Aliyev, A. A., Abbasov, O. R., et al. (2021). Surface structure, activity and microgravimetry modeling delineate contrasted mud chamber types below flat and conical mud volcanoes from Azerbaijan. *Marine and Petroleum Geology*, 134, 105315. <https://doi.org/10.1016/j.marpetgeo.2021.105315>
- Oppo, D. (2012). *Studio dei Vulcani di Fango per la definizione della Migrazione dei Fluidi Profondi* (Dissertation thesis), Dottorato di ricerca in Scienze della terra. Alma Mater Studiorum Università di Bologna, 24 Ciclo. <https://doi.org/10.6092/unibo/amsdottorato/4490>
- Oppo, D., Viola, I., & Capozzi, R. (2017). Fluid sources and stable isotope signatures in authigenic carbonates from the northern Apennines, Italy. *Marine and Petroleum Geology*, 86, 606–619. <https://doi.org/10.1016/j.marpetgeo.2017.06.016>
- Orange, D. L., Greene, H. G., Reed, D., Martin, J. B., McHugh, C. M., Ryan, W. B. F., et al. (1999). Widespread fluid expulsion on a translational continental margin: Mud volcanoes, fault zones, headless canyons, and organic-rich substrate in Monterey Bay, California. *GSA Bulletin*, 111(7), 992–1009. [https://doi.org/10.1130/0016-7606\(1999\)111<0992:WFEOAT>2.3.CO;2](https://doi.org/10.1130/0016-7606(1999)111<0992:WFEOAT>2.3.CO;2)
- Reilly, W. I. (1970). Adjustment of gravity meter observations. *New Zealand Journal of Geology and Geophysics*, 13(3), 697–702. <https://doi.org/10.1080/00288306.1970.10431341>
- Revil, A. (2002). Genesis of mud volcanoes in sedimentary basins: A solitary wave-based mechanism. *Geophysical Research Letters*, 29(12), 1574. 15-1–15-4. <https://doi.org/10.1029/2001GL014465>
- Riffo, A. O., Mauri, G., Mazzini, A., & Miller, S. A. (2021). Tectonic insight and 3-D modelling of the Lusi (Java, Indonesia) mud edifice through gravity analyses. *Geophysical Journal International*, 225(2), 984–997. <https://doi.org/10.1093/gji/ggab020>
- Romano, G., Antonellini, M., Patella, D., Siniscalchi, A., Tallarico, A., Tripaldi, S., & Piombo, A. (2023). Fluid conduits and shallow-reservoir structure defined by geoelectrical tomography at the Nirano Salse (Italy). *Natural Hazards and Earth System Sciences*, 23(8), 2719–2735. <https://doi.org/10.5194/nhess-23-2719-2023>
- Sayyadul, A. (2005). Three-dimensional gravity modelling of a Trinidad mud volcano, West Indies. *Exploration Geophysics*, 36(3), 329–333. <https://doi.org/10.1071/EG05329>
- Sciarrà, A., Cantucci, B., Ricci, T., Tomonaga, Y., & Mazzini, A. (2019). Geochemical characterization of the Nirano mud volcano, Italy. *Applied Geochemistry*, 102, 77–87. <https://doi.org/10.1016/j.apgeochem.2019.01.006>
- Tingay, M. R. P., Hillis, R. R., Swarbrick, R. E., Morley, C. K., & Abdul Razak, D. (2009). Origin of overpressure and pore-pressure prediction in the Baram province, Brunei. *AAPG Bulletin*, 93(1), 51–74. <https://doi.org/10.1306/08080808016>
- Vannoli, P., Martinelli, G., & Valensise, G. (2021). The seismotectonic significance of geofluids in Italy. *Frontiers in Earth Science*, 9. <https://doi.org/10.3389/feart.2021.579390>
- Viganò, A., Della Vedova, B., Ranalli, G., Martin, S., & Scafidi, D. (2012). Geothermal and rheological regime in the Po plain sector of Adria (Northern Italy). *Italian Journal of Geosciences*, 131(2), 228–240. <https://doi.org/10.3301/IJG.2012.09>
- Wang, C., & Manga, M. (2021). *Earthquakes and water. Lecture Notes in Earth System Sciences*. Springer.
- Wang, Y., Lin, Y. N., Ota, Y., Chung, L.-H., Shyu, J. B. H., Chiang, H.-W., et al. (2022). Mud diapir or fault-related fold? On the development of an active mud-cored anticline offshore southwestern Taiwan. *Tectonics*, 41(9). <https://doi.org/10.1029/2022TC007234>
- Zhong, S., Zhang, J., Luo, J., Yuan, Y., & Su, P. (2021). Geological characteristics of mud volcanoes and diapirs in the Northern Continental Margin of the South China Sea: Implications for the mechanisms controlling the genesis of fluid leakage structures. *Geofluids*, 2021, 5519264. <https://doi.org/10.1155/2021/5519264>